Crystal Structures and Properties of Eu_2GeSe_4 and $Eu_2Ge_2Se_5$

M. Tampier[a], D. Johrendt[a], R. Pöttgen[b], G. Kotzyba[b], C. Rosenhahn[c], and B. D. Mosel[c]

[a] Institut für Anorganische Chemie und Strukturchemie, Lehrstuhl II, Heinrich-Heine-Universität Düsseldorf, Universitätsstrasse 1, D-40225 Düsseldorf, Germany
[b] Institut für Anorganische und Analytische Chemie, Universität Münster, Wilhelm-Klemm-Straße 8, D-48149 Münster, Germany
[c] Institut für Physikalische Chemie, Universität Münster, Schloßplatz 4/7, D-48149 Münster, Germany

Reprint requests to D. Johrendt. E-mail: johrendt@uni-duesseldorf.de

Z. Naturforsch. **57 b,** 133–140 (2002); received November 2, 2001

Europium, Selenogermanate, Phase Transition

Europium selenogermanate(IV) and Europium selenogermanate(III) were synthesized by direct reactions of the elements at 1023 K and their crystal structures determined by single crystal methods. α-Eu_2GeSe_4 ($P2_1$, a = 6.964(1), b = 7.055(2), c = 8.400(2) Å, β = 108.12(2)°, Z = 2) crystallizes as a polar variant of the monoclinic Sr_2GeS_4-type at room temperature. At 673 K, the structure is centrosymmetric (β-Eu_2GeSe_4, $P2_1/m$, a = 6.969(1), b = 7.059(2), c = 8.516(2) Å, β = 107.99(2)°, Z = 2), and a phase transition $P2_1 \rightarrow P2_1/m$ as known from Eu_2GeS_4 is highly probable. $Eu_2Ge_2Se_5$ ($P2_1/n$, a = 8.421(4), b = 12.235(4), c = 9.127(3) Å, β = 93.67(4)°, Z = 4) crystallizes in the $Sr_2Ge_2Se_5$ type, mainly characterized by complex $[Ge_4Se_{10}]^{8-}$ anions with homonuclear Ge-Ge bonds. Both compounds are deep red Zintl phases according to $(Eu^{2+})_2Ge^{4+}(Se^{2-})_4$ and $(Eu^{2+})_2(Ge^{3+})_2(Se^{2-})_5$. Magnetic susceptibility measurements show paramagnetic behavior above 20 K with magnetic moments of 8.00(5) μ_B/Eu and 8.10(5) μ_B/Eu, respectively, indicating Eu^{2+}. $Eu_2Ge_2Se_5$ orders antiferromagnetically at T_N = 4.2(2) K and undergoes a metamagnetic transition at 2 K at a critical field of 0.5(3) T. The saturation moment at 2.2 K and 5.5 T is 7.00(2) μ_B/Eu. Eu_2GeSe_4 is a ferromagnet with T_C = 5.8(2) K and a saturation moment at 2.2 K and 5.5 T of 6.92(2) μ_B/Eu. ^{151}Eu Mössbauer spectroscopic measurements of Eu_2GeSe_4 and $Eu_2Ge_2Se_5$ at 78 K show isomer shifts of –12.43(4) mm/s and –12.69(5) mm/s, respectively, in accordance with divalent europium.

Introduction

A variety of ternary europium group 14 sulfides have been reported, including Eu_2MS_4 (M = Si, Ge, Sn) [1, 2, 3], Eu_2MS_5 (M = Ge, Sn) [4, 5] and several thiostannates such as $Eu_2Sn_2S_7$, $Eu_5Sn_3S_{12}$ and $Eu_4Sn_2S_9$ [3]. The silicon and germanium compounds contain exclusively tetrahedral MS_4^{4-} anions while tin also occurs as Sn^{2+} with octahedral environment. Europium is divalent in most cases, but Eu^{3+} was found in the quaternary sulfides $KEuMS_4$ (M = Si, Ge) [6] with a structure closely related to Eu_2MS_4, and in $Eu_5Sn_3S_{12}$ [7]. However, the latter is the only compound of which magnetic data exist. In contrast to the sulfides, homologous selenium compounds remained scarcely investigated. Recently, K_2EuMSe_5 (M = Si, Ge) with MSe_5^{4-} units [6] and Eu_2SnSe_5 containing triselenide ions Se_3^{2-}, were reported [8].

As shown in a previous paper [9], Eu_2GeS_4 undergoes a second order phase transition from a polar (space group $P2_1$) to a centrosymmetric structure (space group $P2_1/m$) at T_C = 335 K, *i. e.* Eu_2GeS_4 is probably a new ferroelectric. We continued our investigation by preparing the analogous selenide in order to establish if Eu_2GeSe_4 crystallizes isotypically with the thiogermanate and in particular whether or not it shows the same structural phase transition. During the synthetic work we discovered the selenogermanate(III) $Eu_2Ge_2Se_5$, whose crystal structure is also reported here. Magnetic measurements and ^{151}Eu Mössbauer spectroscopic experiments were performed of both compounds in order to clarify the valence state of europium.

Experimental Section

Powder samples of Eu_2GeSe_4 and $Eu_2Ge_2Se_5$ were synthesized from the elements (purity > 99.5%) in two

Table 1. Crystal data and structure refinements for α-Eu_2GeSe_4, β-Eu_2GeSe_4 and $Eu_2Ge_2Se_5$.

Compound	α-Eu_2GeSe_4	β-Eu_2GeSe_4	$Eu_2Ge_2Se_5$
Temperature [K]	298	673	298
Empirical formula	Eu_2GeSe_4	Eu_2GeSe_4	$Eu_2Ge_2Se_5$
Molar mass [g/mol]	692.35	692.35	842.74
Lattice parameters [Å,°]	a = 6.964(1)	a = 6.969(1)	a = 8.421(4)
	b = 7.055(2)	b = 7.059(2)	b = 12.235(4)
	c = 8.400(2)	c = 8.516(2)	c = 9.127(3)
	β = 108.12(2)	β = 107.99(2)	β = 93.67(4)
	V = 392.26	V = 398.32	V = 951.6
Crystal system	monoclinic	monoclinic	monoclinic
Space group	$P2_1$	$P2_1/m$	$P2_1/n$
Formula units per cell	Z = 2	Z = 2	Z = 4
Calculated density [g/cm^3]	5.86	5.77	5.96
Transmission ratio (max/min)	5.48	6.20	6.07
Absorption coefficient [mm^{-1}]	μ = 38.05	μ = 37.47	μ = 38.83
Detector distance [mm]	50	60	50
Exposure time [min]	3	3	3.5
ϕ Range; increment [°]	0-200; 2.4	0-250; 2.0	0-182; 1.4
Profile / pixel	9-21	9-21	9-19
ϑ Range for data collection [°]	3-30	3-28	3-30
Range in *hkl*	±9, ±9, ±11	±9, ±9, ±11	±11, ±17, ±12
Completeness of data set [%]	99.6	99.1	99.6
Total no. reflections	4522	5285	10052
Independent reflections	2317 (R_{int} = 0.056)	1056 (R_{int} = 0.12)	2794 (R_{int} = 0.16)
Reflections with $F_O > 4\sigma(F_O)$	1448	362	1144
Parameter	65	41	83
Goodness-of-fit on F^2	0.800	0.619	0.697
$R1$ indices ($F_O > 4\sigma(F_O)$)	$R1$ = 0.039	$R1$ = 0.041	$R1$ = 0.055
$wR2$ Indices (all data)	$wR2$ = 0.095	$wR2$ = 0.097	$wR2$ = 0.126
BASF parameter	0.46(9)	–	–
Largest diff. peak / hole [e/Å^3]	1.75 / –1.55	1.44 / –1.92	2.00 / –4.49

steps. (i) Binary compounds Eu_2Ge and EuGe were prepared by heating stochiometric mixtures of europium metal and germanium powder at 1123 K for 10 h in alumina crucibles sealed in quartz glass ampoules under an argon atmosphere. (ii) After homogenization in an argon filled glove box, both products were oxidized by stochiometric amounts of selenium at 1023 K for 15 h. The samples were homogenized again and reheated to 1023 K for 50 h. This procedure resulted in deep red powders of Eu_2GeSe_4 and $Eu_2Ge_2Se_5$, respectively. Both compounds are stable in air and insoluble in common organic solvents. X-ray powder patterns (HUBER G600, Cu-K_α, silicon as external standard) could be indexed completely by using the monoclinic cell parameters obtained from the single crystal experiments. The correct hkl assignments were checked by intensity calculations [10] using the atomic positions from the structure refinements.

Small irregularly shaped crystals (diameter ≈ 0.07 mm) were selected directly from the samples and carefully inspected by Weissenberg photographs (Cu-K_α). For the high temperature data collections with Eu_2GeSe_4, the crystal was fixed in the narrow part of a quartz capillary (diameter 0.2 mm), which was evacuated, sealed under argon atmosphere and mounted on STOE and NONIUS crystal heater equipments.

X-ray intensity data of Eu_2GeSe_4 were collected at 298 K and 673 K and of $Eu_2Ge_2Se_5$ at 298 K on a STOE image plate system (IPDS). Additional unique data sets of Eu_2GeSe_4 were measured at 373 and 523 K on a Siemens $P2_1/P3$ 4-circle diffractometer. Graphite monochromatized Mo$K\alpha$ radiation was used throughout. The IPDS and P3 software [11, 12] were used for data collection, and X-RED [13] for further processing and numerical absorption corrections. The crystal shapes were obtained on the diffractometer by using the FACEIT video system [14] and carefully optimized by the X-SHAPE [15] software.

Atomic coordinates of the Sr_2GeS_4 structure (space group $P2_1/m$) [16] were initially used for the structure determination of Eu_2GeSe_4. First cycles yielded a residual $R1$ of 0.14 and extremely large displacement parameters U_{22} of the Eu- and Se-atoms on the special position 2*e* (x, $^1/_4$, z). After changing the space group to $P2_1$, the calculations converged to $R1$ = 0.039 with acceptable displacement parameters. Owing to a Flack parameter of

Table 2. Atomic coordinates and isotropic equivalent displacement parameters (pm^2) for α-Eu_2GeSe_4, β-Eu_2GeSe_4 and $Eu_2Ge_2Se_5$.

Atom	Site	*x*	*y*	*z*	U_{eq}
α-Eu_2GeSe_4 (space group $P2_1$)					
Eu1	*2a*	0.7238(1)	0.2231(4)	0.0551(1)	222(2)
Eu2	*2a*	0.7554(1)	0.2138(3)	0.5642(1)	243(3)
Ge	*2a*	0.2725(2)	0.2500*	0.1968(2)	182(4)
Se1	*2a*	0.0895(3)	0.2885(4)	–0.0864(2)	262(5)
Se2	*2a*	0.0807(3)	0.2748(4)	0.3820(2)	285(5)
Se3	*2a*	0.4795(4)	–0.0199(4)	0.2524(3)	226(5)
Se4	*2a*	0.5175(3)	0.4910(4)	0.2636(3)	205(5)
β-Eu_2GeSe_4 (space group $P2_1/m$)					
Eu1	*2e*	0.7237(2)	$^1/_4$	0.0539(2)	470(6)
Eu2	*2e*	0.7582(2)	$^1/_4$	0.5653(2)	529(7)
Ge	*2e*	0.2741(4)	$^1/_4$	0.1982(4)	313(7)
Se1	*2e*	0.0972(4)	$^1/_4$	–0.0832(4)	653(14)
Se2	*2e*	0.0809(4)	$^1/_4$	0.3796(4)	633(13)
Se3	*4f*	0.4992(3)	–0.0061(4)	0.2592(3)	414(5)
$Eu_2Ge_2Se_5$ (space group $P2_1/n$)					
Eu1	*4e*	0.0434(2)	0.1625(1)	0.0302(1)	241(3)
Eu2	*4e*	0.5588(2)	0.3040(1)	0.0208(1)	245(3)
Ge1	*4e*	0.4934(3)	0.0505(2)	0.3351(3)	215(5)
Ge2	*4e*	0.7999(3)	0.4796(2)	0.3131(2)	188(5)
Se1	*4e*	0.2032(3)	0.4423(2)	0.4556(2)	225(5)
Se2	*4e*	0.5360(3)	0.5076(2)	0.2157(3)	220(5)
Se3	*4e*	0.3136(3)	0.2133(2)	0.7913(2)	215(5)
Se4	*4e*	0.1590(3)	0.4104(2)	0.0591(3)	225(5)
Se5	*4e*	0.3423(3)	0.2057(2)	0.2780(2)	212(5)

* fixed.

0.46(9), the last cycles were performed with regard to twin domains, convertible by inversion. Refinements of the data sets measured at 373 and 523 K converged to $R1$ = 0.044 and 0.082, respectively. By using the data collected at 673 K, we obtained *y*-coordinates very close to $^1/_4$ for Eu1, Eu2, Se1 and Se2 with large standard deviations. This clearly indicated a transition to space group $P2_1/m$, which was successfully used for subsequent cycles to a final $R1$ = 0.041.

The unit cell dimensions of $Eu_2Ge_2Se_5$ and the extinction rules indicate the structure to be isotypic to $Sr_2Ge_2Se_5$, space group $P2_1/n$. Refinements with these atomic positions as starting values converged rapidly to $R1$ = 0.055.

Crystallographic data and experimental details for the data collections are listed in Table 1, final atomic positions with equivalent isotropic displacement parameters in Table 2. Important interatomic distances and bond angles are given in Table 3. Further details on the structure determinations may be obtained from: Fachinformationszentrum Karlsruhe, D-76344 Eggenstein-Leopoldshafen (Germany), by quoting the Registry No's. CSD-412227 (α-Eu_2GeSe_4), CSD-412228 (β-Eu_2GeSe_4) and CSD-412229 ($Eu_2Ge_2Se_5$).

The magnetic susceptibilities of polycrystalline samples of Eu_2GeSe_4 and $Eu_2Ge_2Se_5$ were measured with a SQUID magnetometer (MPMS, Quantum Design, Inc.) between 2 and 300 K with magnetic flux densities up to 5.5 T.

The 21.53 keV transition of ^{151}Eu with an activity of 130 MBq (2% of the total activity of a ^{151}Sm:EuF_3 source) was used for the Mössbauer spectroscopic experiments. The measurements were performed with a commercial helium bath cryostat. The temperature of the absorber could be varied from 4.2 to 300 K measured with a metallic resistance thermometer with a precision better than $\pm$0.5 K. The source was kept at room temperature. The material for the Mössbauer spectroscopic investigation was the same as for the susceptibility measurements. The sample was placed in a thin-walled PVC container with a thickness corresponding to about 10 mg Eu/cm^2.

Results and Discussion

Crystal structures and phase transition of Eu_2GeSe_4

α-Eu_2GeSe_4 crystallizes in the α-Eu_2GeS_4 structure at room temperature. This polar variant (space group $P2_1$) can be derived from the Sr_2GeS_4-type (space group $P2_1$/m) by small shifts of certain atomic positions away from the $P2_1$/m mirror planes at $y = {}^1/_4$ and $^3/_4$. Eu^{2+} and Se^{2-} ions move anti-distortive, *i. e.* y(Eu) < $^1/_4$ and y(Se) > $^1/_4$ (see Table 2). Consequently, Eu_2GeSe_4 is expected to have a permanent dipole moment at room temperature. The typical asymmetric sevenfold coordination of europium is depicted in Fig. 1. Six selenium atoms

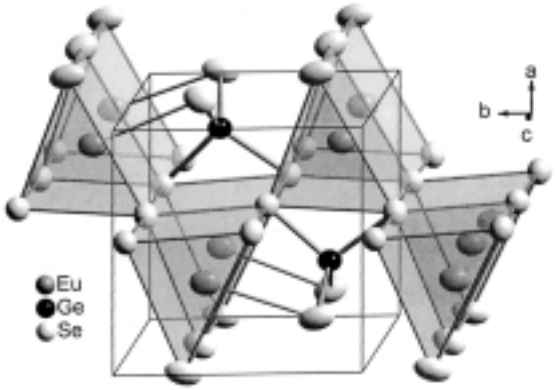

Fig. 1. Crystal structure of α-Eu_2GeSe_4 at 298 K with ellipsoids of 90% probability.

Table 3. Selected interatomic distances (Å) and bond angles (°) in the structures of α-Eu_2GeSe_4, β-Eu_2GeSe_4 and $Eu_2Ge_2Se_5$.

α-Eu_2GeSe_4 (space group $P2_1$)							
Eu1-Se2	3.099(2)	Eu2-Se2	3.133(2)	Ge-Se1	2.339(3)	Se1-Ge-Se3	113.8(1)
Se3	3.113(3)	Se4	3.144(2)	Se3	2.346(3)	Se1-Ge-Se4	106.5(1)
Se4	3.142(3)	Se1	3.171(2)	Se4	2.350(3)	Se3-Ge-Se4	100.6(1)
Se1	3.161(2)	Se3	3.185(3)	Se2	2.351(2)	Se2-Ge-Se1	115.0(1)
Se4	3.205(2)	Se3	3.186(3)			Se2-Ge-Se3	111.7(1)
Se3	3.215(3)	Se4	3.216(3)			Se2-Ge-Se4	107.9(1)
Se1	3.308(3)	Se2	3.283(3)				
Se1	4.179(3)	Se2	4.105(3)				
β-Eu_2GeSe_4 (space group $P2_1/m$)							
Eu1-Se2	3.102(4)	Eu2-Se2	3.123(3)	Ge-Se1	2.332(5)	Se2-Ge-Se1	116.7(1)
Se3	3.150(3) 2x	Se3	3.174(3) 2x	Se2	2.347(4)	Se3-Ge-Se3	100.0(2)
Se1	3.164(3)	Se1	3.189(4)	Se3	2.344(3) 2x	Se1-Ge-Se3	109.4(1)2x
Se3	3.234(3) 2x	Se3	3.227(3) 2x			Se2-Ge-Se2	109.6(1)2x
Se1	3.726(1) 2x	Se2	3.689(1) 2x				
$Eu_2Ge_2Se_5$ (space group $P2_1/n$)							
Eu1-Se2	3.101(3)	Eu2-Se3	3.054(3)	Se4- Ge1-Se5	112.2(1)		
Se1	3.173(3)	Se2	3.074(3)	Ge2-Ge1-Se5	124.6(1)		
Se4	3.191(3)	Se3	3.173(3)	Ge2-Ge1-Se4	113.1(1)		
Se5	3.205(3)	Se2	3.223(3)	Se4- Ge1-Se2	107.6(1)		
Se3	3.310(3)	Se5	3.291(3)	Se4- Ge1-Se3	95.4(1)		
Se5	3.317(3)	Se1	3.317(3)	Se4- Ge1-Se1	98.3(1)		
Se1	3.434(3)	Se5	3.362(3)				
Se3	3.511(3)	Se4	3.647(3)	Se2- Ge2-Se1	102.6(1)		
				Se3- Ge2-Se1	119.3(1)		
Ge1 Se5	2.326(3)	Ge2 Se1	2.319(3)	Se3- Ge2-Se2	99.3(1)		
Se4	2.383(3)	Se2	2.365(3)	Ge1-Ge2-Se5	114.2(1)		
Se4	2.471(3)	Se3	2.372(3)	Ge1-Ge2-Se6	115.4(1)		
Ge2	2.431(3)	Ge1	2.431(3)	Ge1-Ge2-Se4	105.6(1)		

form a trigonal prism (Eu-Se distances from 3.099 to 3.216 Å) and one is located over a rectangular face at a distance of 3.308 Å. The selenium atoms which are located over the other prism faces at distances larger then 4.2 Å cannot be considered as coordinated to europium. The $EuSe_{2/2}Se_{4/4}$ prisms are connected *via* common triangular faces along *c* and share edges in *b* direction (see Fig. 1). Germanium is in almost regular tetrahedral coordination of four selenium atoms. The mean Ge-Se distance of 2.347 Å is slightly shorter than the sum of Pauling's tetrahedral radii of 2.36 Å (Ge: 1.22 Å, Se: 1.14 Å) [17], indicating strong covalent bonding. Se-Ge-Se bond angles of the $GeSe_4$ tetrahedra differ by less than 10% from 109.4°. Regarding these results we can describe the structure as a dense packing of $GeSe_4^{4-}$ tetrahedral anions, separated and charge balanced by Eu^{2+} cations.

Fig. 2 shows the temperature dependences of the *y*-coordinates of Eu1, Eu2, Se1 and Se2 in

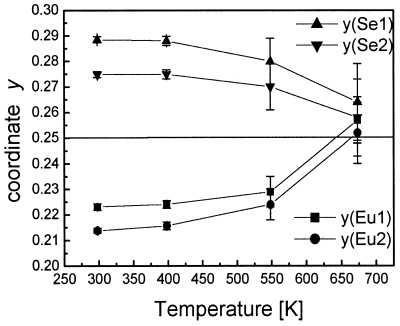

Fig. 2. Atomic *y*-coordinates of Eu1, Eu2, Se1 and Se2 at different temperatures (space group $P2_1$). The error bars represent $3\sigma(y)$, respectively.

Eu_2GeSe_4, each obtained from structure refinements in the space group $P2_1$. The deviations from $^1/_4$ decrease with increasing temperature and the values for T = 673 K are very close to $^1/_4$ with large standard deviations. This result indicates a continuous (second order) $P2_1 \rightarrow P2_1/m$ transition as re-

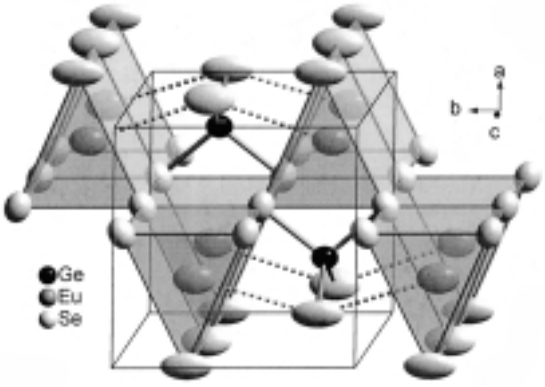

Fig. 3. Crystal structure of β-Eu_2GeSe_4 at T = 673 K with ellipsoids of 90% probability.

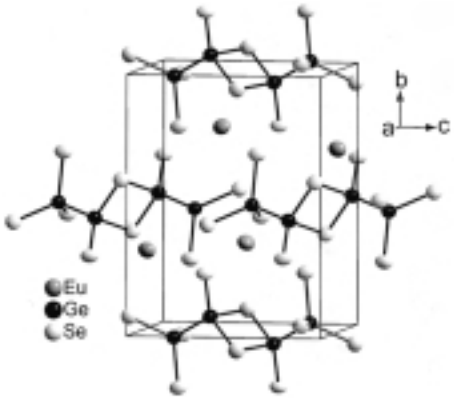

Fig. 4. Crystal structure of $Eu_2Ge_2Se_5$. The $[Ge_4Se_{10}]^{8-}$ anions are emphasized.

ported for Eu_2GeS_4 [9] and allows to estimate a T_C of about 600 - 650 K.

The crystal structure of β-Eu_2GeSe_4 at 673 K is shown in Fig. 3. Its atomic arrangement meets the $P2_1/m$ space group symmetry from the view of the X-ray method. In particular the Eu1, Eu2, Se1 and Se2 atoms appear to be located at special positions $2e$ (x, $^1/_4$, z) on average, but relatively large U_{22} displacement parameters of Se1 and Se2 perpendicular to the mirror planes indicate a substantial disorder of these atoms (see thermal ellipsoids in Fig. 3). This result is, apart from a higher transition temperature, the same as already reported for the isostructural sulfide: Eu_2GeS_4 shows a structural phase transition from a polar α-phase (space group $P2_1$) to a centrosymmetric high temperature β-phase (space group $P2_1/m$) at T_C = 335 K. Main contributions to this transition are antidistortive shifts of sulfide (corresponding to Se1 and Se2 in Eu_2GeSe_4) and europium ions. This behavior can be understood as a condensed optical phonon mode with A_u symmetry. Since the high temperature structures of Eu_2GeSe_4 at 673 K and of Eu_2GeS_4 above 335 K are almost identical, we can assume that the selenide reported herein will show the same type of phase transition. However, the exact T_C and details of the transition mechanism of Eu_2GeSe_4 have to be examined by further temperature dependent measurements, which we intend to report in a forthcoming paper.

From the viewpoint of X-ray diffraction data, the coordination number of europium changes from 7 to 6(+2) during the transition (see Table 3), but this is a matter of a dynamic effect, since the Se1 and Se2 atoms in β-Eu_2GeSe_4 move in double minimum potentials along their y-coordinates with energy maxima at y = $^1/_4$. Because these movements are orders of magnitudes faster than the duration of a diffraction intensity measurement, the X-ray method can only give average atomic positions.

Crystal structure of $Eu_2Ge_2Se_5$

$Eu_2Ge_2Se_5$ crystallizes isotypically to the recently reported $Sr_2Ge_2Se_5$ [18] and is only briefly discussed here. As seen from Fig. 4, the structure is built up from complex $[Ge_4Se_{10}]^{8-}$ anions, orientated approximately along [101]. This anion may be regarded as two ethane-like Se_3Ge-$GeSeSe_{2/2}$ fragments sharing two selenium atoms. As expected, the geometries of the $[Ge_4Se_{10}]^{8-}$ anion in $Eu_2Ge_2Se_5$ and $Sr_2Ge_2Se_5$ are almost the same.

Germanium is surrounded tetrahedrally by three selenium and one germanium atom with Ge-Se bond lengths ranging from 2.319(3) to 2.372(3) Å for the terminal Se atoms and from 2.383(3) to 2.471(3) Å for the bridging ones. The Ge-Ge distance is 2.431(3) Å in agreement with the covalent radius of 1.22 Å [17]. Eight selenium atoms coordinate the europium atoms forming distorted bicapped trigonal prisms or distorted square antiprisms. Eu-Se distances range from 3.054(3) to 3.647(3) Å.

The formal oxidation state of germanium in $Eu_2Ge_2Se_5$ is Ge^{3+} because of the formation of homonuclear Ge-Ge bonds. This leads to an electron precise ionic formula splitting $(Eu^{2+})_2(Ge^{3+})_2(Se^{2-})_5$ in agreement with the red color and transparency of the crystals.

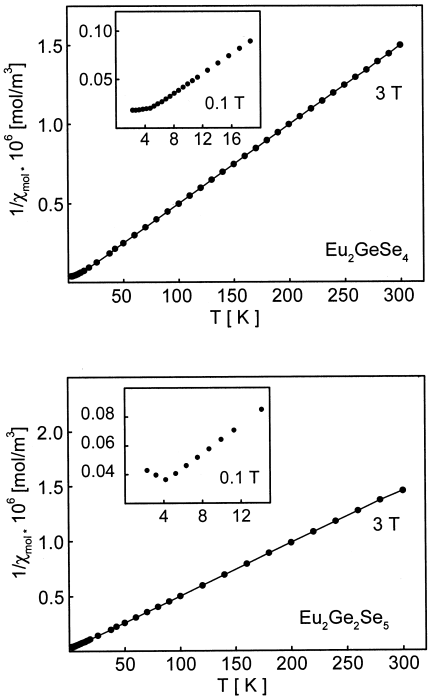

Fig. 5. Temperature dependence of the inverse magnetic susceptibilities of Eu_2GeSe_4 and $Eu_2Ge_2Se_5$ determined at an external field of B = 3 T. The inserts show the low temperature behavior measured at B = 0.1 T.

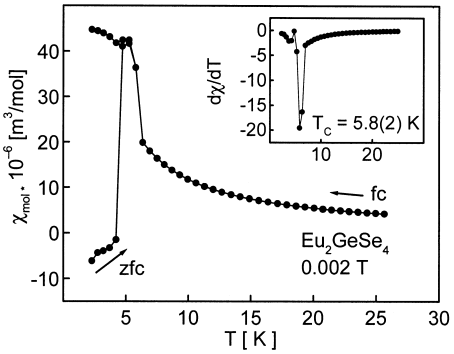

Fig. 6. Low temperature susceptibility (zero-field-cooling *ZFC* and field-cooling *FC* modus) of Eu_2GeSe_4 at 0.002 T (kink-point measurement). The insert shows the derivative $d\chi/dT$ of the *FC* curve with a sharp peak at T_C = 5.8(2) K.

Magnetic properties

The temperature dependence of the inverse magnetic susceptibilities (3 T measurement) of Eu_2GeSe_4 and $Eu_2Ge_2Se_5$ is presented in Fig. 5. Eu_2GeSe_4 shows Curie behavior above 20 K with a magnetic moment of 8.00(5) μ_B/Eu, close to the value of 7.94 μ_B for the free Eu^{2+} ion. The low temperature behavior shown in the insert of Fig. 5 indicates ferromagnetic ordering for Eu_2GeSe_4. The precise Curie temperature of 5.8(2) K was determined from the derivative $d\chi/dT$ (insert of Fig. 6) of low-temperature low-field measurements as outlined in Fig. 6 (zero-field and field-cooling (kink point) curves).

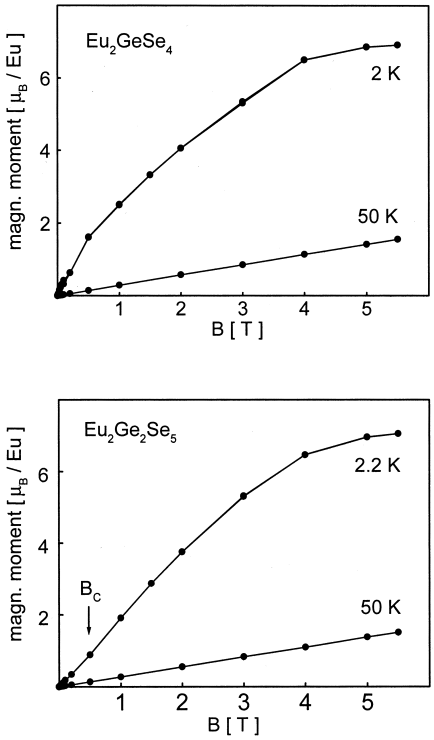

Fig. 7. Field-dependence of the magnetic moment per europium atom of Eu_2GeSe_4 and $Eu_2Ge_2Se_5$ at different temperatures. The critical field B_C for $Eu_2Ge_2Se_5$ is marked by a small arrow.

The inverse susceptibility of $Eu_2Ge_2Se_5$ (Fig. 5) shows a slight curvature indicating a small temperature independent contribution. The data above 20 K were therefore fitted with a modified Curie-Weiss expression $\chi = \chi_O + C/(T - \Theta)$ resulting in a paramagnetic Curie temperature (Weiss constant) of –4(1) K, an experimental magnetic moment of 8.10(5) μ_B/Eu and a temperature independent contribution of $\chi_O = 1.1(1) \times 10^{-9}$ m^3/mol. At 0.1 T antiferromagnetic ordering at T_N = 4.2(2) K is detected (insert in Fig. 5).

In Fig. 7 we present the magnetization behavior of both compounds. At 50 K, well above the magnetic ordering temperatures, the magnetization

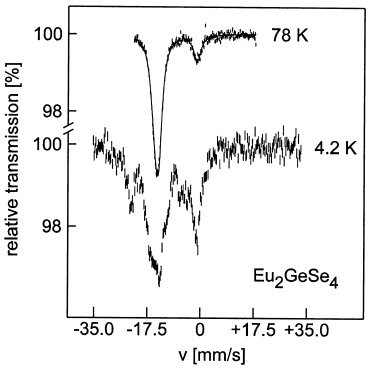

Fig. 8. Experimental and simulated ^{151}Eu Mössbauer spectra of Eu_2GeSe_4 at different temperatures.

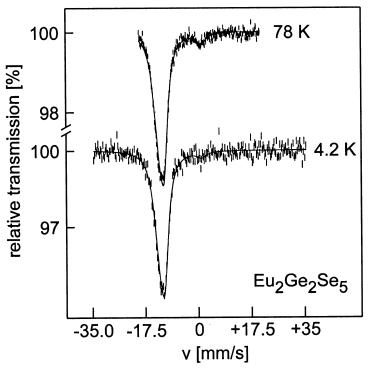

Fig. 9. Experimental and simulated ^{151}Eu Mössbauer spectra of $Eu_2Ge_2Se_5$ at different temperatures.

curves of both selenogermanates are almost linear as expected for paramagnetic compounds. At 2 K the magnetization curve of Eu_2GeSe_4 increases and tends to saturate at a field strength of about 4 T. At the highest obtainable field strength of B = 5.5 T the magnetization reaches a value of 6.92(2) μ_B/Eu at 2 K, near the theoretical saturation magnetization of 7.0 μ_B/Eu, indicating full parallel spin alignment. The magnetization curve of $Eu_2Ge_2Se_5$ at 2.2 K looks quite similar, however, up to the critical field of 0.5(3) T we observe an almost linear increase and then a stronger increase. This may be ascribed to a metamagnetic (antiparallel to parallel spin alignment) or spin-flip transition, although the transition point (critical field) is not very pronounced. At 2.2 K and 5.5 T the magnetization saturates at a value of 7.00(2) μ_B/Eu, similar to Eu_2GeSe_4.

^{151}Eu Mössbauer spectroscopy

The ^{151}Eu Mössbauer spectra of Eu_2GeSe_4 and $Eu_2Ge_2Se_5$ at 78 and 4.2 K are presented in Figs. 8 and 9 together with transmission integral fits. At 78 K, well above the magnetic ordering temperatures we observe single signals at isomer shifts of δ = –12.43(4) mm/s (Eu_2GeSe_4) and –12.69(5) mm/s ($Eu_2Ge_2Se_5$), indicating divalent europium. The highly negative isomer shifts reflect the ionic character of these selenogermanates. In all spectra a Eu(III) impurity was detected around δ = 1 mm/s and included in the fits by a simple Lorentzian. The fractional area of this component was 4% for $Eu_2Ge_2Se_5$ and 15% for Eu_2GeSe_4. We attribute this behavior to a partial oxidation of the samples during the Mössbauer experiments and not to a mixed-valence effect, since the magnetic data clearly show a Eu^{2+} ground state. The experimental line widths of Γ = 2.4 mm/s (Eu_2GeSe_4) and Γ = 2.9(2) mm/s ($Eu_2Ge_2Se_5$) are close to the usual line width of 2.3 mm/s for ^{151}Eu. The electric field gradient is 7.7(6) mm/s for Eu_2GeSe_4 and 11.2 mm/s for $Eu_2Ge_2Se_5$. Values without standard deviations were kept fixed during the fitting procedure.

Just at the Néel temperature of 4.2 K, the ^{151}Eu spectrum of $Eu_2Ge_2Se_5$ shows only a small increase of the line width (3.1(5) mm/s), most likely indicating the beginning of magnetic hyperfine interactions. At lower temperatures we expect a larger hyperfine field splitting. The 4.2 K spectrum of Eu_2GeSe_4 (Fig. 8) is very complex. Since this spectrum was recorded only slightly below the Curie temperature of 5.8(2) K, the hyperfine field at the europium nuclei is still small. At lower temperatures larger hyperfine fields are expected. Due to the poor signal-to-noise ratio and the relatively broad signals, a theoretical fit of this spectrum was not reasonable to be carried out.

Acknowledgements

We thank Prof. A. Mewis and Prof. W. Frank for their interest and financial support. Thanks go to PD Dr. M. Wickleder for the HT-IPDS measurement. We are also grateful to Prof. W. Jeitschko and Prof. H. Eckert for the permission to use their SQUID magnetometer and Mössbauer equipment. This work was financially supported by the Fonds der Chemischen Industrie and the Deutsche Forschungsgemeinschaft (Jo257/3, Po573/1-4).

[1] D. Johrendt, R. Pocha, Acta Crystallogr. **E57**, i57 (2001).
[2] G. Bugli, J. Dugue, S. Barnier, Acta Crystallogr. **B35**, 2690 (1979).
[3] J. Flahaut, P. Larunelle, M. Guittard, S. Jaulmes, M. Julien-Pouzol, C. Lavenant, J. Solid State Chem. **29**, 125 (1979).
[4] I. O. Nasibov, T. I. Sultanov, T. A. Dzhalizade, Zh. Neorg. Khim. **26**, 2529 (1981).
[5] S. Jaulmes, M. Joulien-Pouzol, P. Laruelle, M. Guittard, Acta Crystallogr. **B38**, 79 (1982).
[6] C. R. Evenson, P. K. Dorhout, Inorg. Chem. **40**, 2409 (2001).
[7] T. I. Volkonskaya, A. G. Gorobets, S. A. Kizhaev, I. A. Smirnov, V. V. Tikhonov, M. Guittard, C. Lavenant, J. Flahaut, Phys. Stat. Sol. **A57,** 731 (1980).
[8] C. R. Everson, P. K. Dorhout, Z. Anorg. Allg. Chem. **524**, 83 (2001).
[9] M. Tampier, D. Johrendt, J. Solid State Chem. **158**, 343 (2001).
[10] W. Kraus, G. Nolze, PowderCell for Windows Version 2.3, BAM, Federal Institute for Materials Research and Testing, Berlin (1999).
[11] STOE IPDS Software, Rev. 2.93, (STOE & Cie GmbH (2000).
[12] P3-Software, © Siemens Analytical Xray Instr. Inc., Madison, USA (1980).
[13] X-RED data reduction for Stadi4 and IPDS, Rev. 1.19, (STOE & Cie GmbH (1999).
[14] Faceit Video System, (STOE & Cie GmbH (1998).
[15] X-SHAPE, Crystal optimization for numerical absorption correction, Rev. 1.06, (STOE & Cie GmbH (1999).
[16] E. Philippot, M. Ribes, M. Maurin, Rev. Chim. Mineral. **8**, 99 (1971).
[17] L. Pauling, Die Natur der chemischen Bindung, 3. Aufl., p. 237, Verlag Chemie, Weinheim 1976.
[18] D. Johrendt, M. Tampier, Chem. Eur. J. **6**, 994 (2000).